

Article

An Incentive-Based Mechanism to Enhance Energy Trading among Microgrids, EVs, and Grid

Muhammad Ahsan Khan ¹, Akhtar Hussain ², Woon-Gyu Lee ¹  and Hak-Man Kim ^{1,3,*} 

¹ Department of Electrical Engineering, Incheon National University, 119 Academy-ro, Yeonsu-gu, Incheon 22012, Republic of Korea; ahsan1996@inu.ac.kr (M.A.K.); dltnlqpf@inu.ac.kr (W.-G.L.)

² Department of Electrical and Computer Engineering, University of Alberta, Edmonton, AB T6G 2R3, Canada; akhtar3@ualberta.ca

³ Research Institute for Northeast Asian Super Grid, Incheon National University, 119 Academy-ro, Yeonsu-gu, Incheon 22012, Republic of Korea

* Correspondence: hmkim@inu.ac.kr; Tel.: +82-32-835-8769

Abstract: The growing penetration of electric vehicles (EVs) introduces both opportunities and challenges for power grid operators. Incentivization is considered a viable option to tempt EV owners to participate in supporting the grid during peak load intervals while receiving compensation for their services. Therefore, this study proposes a two-step incentive mechanism to reduce the peak load of the grid by enabling power trading among the microgrid, EVs and the utility grid. In the first step, an incentive price is determined for EVs considering the grid-loading conditions during different hours of the day. In the second step, a multi-objective optimization problem is formulated to optimize trading among different entities, such as EVs, the microgrid and the utility grid. The two objectives considered in this study are the operation cost of the microgrid and the revenue of EVs. Monte Carlo simulations are used to deal with uncertainties associated with EVs. Simulations are conducted to analyze the impact of different weight parameters on the energy-trading amount and operation cost of EVs and MG. In addition, a sensitivity analysis is conducted to analyze the impact of changes in the EV fleet size on the energy-trading amount and operation cost.

Keywords: electric vehicles; energy trading; equipment overload; incentive price; microgrid; multi-objective optimization



Citation: Khan, M.A.; Hussain, A.; Lee, W.-G.; Kim, H.-M. An Incentive-Based Mechanism to Enhance Energy Trading among Microgrids, EVs, and Grid. *Energies* **2023**, *16*, 6359. <https://doi.org/10.3390/en16176359>

Academic Editors: Omar Ali Beg, Zongjie Wang and Shan Zuo

Received: 27 July 2023

Revised: 21 August 2023

Accepted: 31 August 2023

Published: 1 September 2023



Copyright: © 2023 by the authors. Licensee MDPI, Basel, Switzerland. This article is an open access article distributed under the terms and conditions of the Creative Commons Attribution (CC BY) license (<https://creativecommons.org/licenses/by/4.0/>).

1. Introduction

Carbon emissions have been a major challenge for different sectors, including transportation, during the last few decades [1]. Several countries have ambitious plans to reduce emissions, such as net-zero emissions by 2050 [2]. It has been reported that the transportation sector contributes to carbon emissions by about 24% [3]. Electric vehicles (EVs) can aid in the decarbonization of transportation, as they produce lesser emissions throughout their life cycle as compared to combustion engine-based vehicles [4]. To reach the net-zero emissions goal by 2050, it is estimated that approximately 60% of worldwide new car sales must consist of electric vehicles by the year 2030 [5]. As the number of EVs on the roads grows, so does the demand for energy. At present, EVs account for roughly 0.3% of worldwide energy consumption. This figure is projected to rise to between 2% and 4% by the year 2030 [6]. According to [7], with the increment of 10% of the EVs penetration, up to 5% of the load demand from the grid increases. The increase in electricity demand may adversely impact the grid equipment and result in overloading.

To minimize this impact, vehicle-to-grid (V2G) technology has been introduced. Under the V2G framework, EVs can provide stored energy back to the grid [8]. V2G is beneficial for society and individuals, as it can flatten the grid load, and it can be a source of income for EV owners by selling the stored energy [9]. V2G is currently being practiced in different parts of the world [10]. An overview of V2G technology, highlighting the progress made so

far and identifying the future challenges, is presented in [11]. The successful adoption of V2G service is not only dependent on the development of technology but also the willingness of EV owners to take part and utilize this technology [12]. The study [13] explored the perceptions and attitudes of EV owners towards the adoption of V2G technology at workplaces. EV owners may be concerned about battery degradation due to continuous charging and discharging that hinders the adoption of the V2G service. It was demonstrated in [14] that frequent charging and discharging for the V2G service result in battery degradation and life cycle shortening. Thus, some effective mechanism should offset the cost of battery degradation and motivate EV owners to provide the V2G service. A computational model of EVs with battery degradation was examined in the study [15]. The results reveal the benefits of V2G technology, allowing EV owners to make a profit by outweighing the costs related to battery degradation. The study evaluates the time-of-use (TOU) pricing in [16], where EV owners are provided with an incentive to charge EVs during off-peak intervals. A profit maximization problem for EV owners to sell their excess energy is formulated in [17]. In [18,19], control algorithms are proposed to maximize the profit for EV owners by selling power to the grid. The EV charging coordination is analyzed by Yao et al. [20] based on the incentive and price-based demand response. Moreover, a linear optimization model to maximize the profit obtained by EV aggregators, including grid services is formulated in [21]. Similarly, a linear planning model is introduced to assist EV aggregators to participate in the ancillary service market in [22]. This model also determines the optimal incentives for EV owners. In addition to V2G, vehicle-to-everything (V2X) is used to create new opportunities for EV owners to generate revenue through participation in grid services [23,24].

Meanwhile, microgrids (MGs) can also participate in energy markets to trade electricity with the grid. MGs and EVs can be integrated to further enhance the local power trading and serve as energy storage in MG [25,26]. This integration forms part of an energy-management framework for communities that includes multiple independent energy storage system service providers, and it requires a cost-effective energy flow management among them [27,28]. Several studies have considered the integration of EVs with the MG system [29–31]. This is especially beneficial for commercial buildings, where several EVs are parked at a time [32], for example, from 9:00 a.m. to 6:30 p.m. [33]. In [34], vehicle-to-MG (V2M) is realized considering different EV architectures. A two-stage optimization framework is purposed for EVs to provide ancillary services to MG in [35]. The major objectives considered in this study are to minimize fluctuations in the MG load, maximize the use of renewable energy, and maximize the benefits to EV users. In [36], a two-stage optimization framework is proposed to integrate large-scaled EV fleets with MGs. The MG dispatch center develops a cluster-based day-ahead optimal EV charging/discharging strategy. This strategy aims to reduce costs for both the MG operator and EV owners. A multi-objective optimization framework that considers EV owners' participation in V2M and carbon emission cost is proposed in [37].

Recently, the concept of internal trading was introduced to facilitate trading among MGs and other local entities. Internal trading is beneficial for both local entities and the grid. For local entities, it provides a better price for trading power locally as compared to the grid. Similarly, it can reduce the dependence of MGs on the grid, thus relieving the external grid during peak load intervals [38]. In [39], a centralized energy management system (EMS) is formulated for the optimization of internal trading between MGs. I.A. Umoren et al. [40] use blockchain technology to enable peer-to-peer energy trading between EVs and MGs in a local network, utilizing the capabilities offered by the 5G network. In [41], the author investigates local energy market structures, their mechanisms, and participants, along with an analysis of the existing infrastructure's challenges and prospective research directions in the field.

It can be observed from the literature survey that plenty of literature exists on enabling energy trading among local entities and with the grid. However, there are a limited number of studies on incentivizing EVs to participate in V2G services and to compensate them for

battery degradation. Additionally, the reluctance of EV owners to share private information, such as vehicle details, arrival, departure, or battery status adds a layer of complexity. This underscores the need for an effective incentive mechanism that both encourages EV owners to engage in V2G services, thereby alleviating the grid load during peak demand, and assists in offsetting the costs related to EV ownership. Importantly, this mechanism should have minimum dependence on private information from the EV owners. Furthermore, with the inclusion of internal trading and incentivized pricing, a complex trading structure can emerge among entities, such as the utility grid, EVs, and the MG that need to be explored. In addition, the objectives of EV fleets and microgrids could be different due to differences in ownership. Consequently, there is a need for an effective model that can adeptly capture this complexity and offer optimal solutions based on the preferences of the diverse stakeholders involved.

To overcome the limitations of existing studies, a trading framework is proposed in this study that incorporates an incentivized selling price for EV owners to promote the voluntary participation and ensures that EV owners get compensated for the price of their involvement in V2G services; also, it does not depend on any sensitive information related to EV owners. Our proposed analysis addresses the trading mechanism among different entities, such as microgrids, EVs, and the utility grid. It employs a mixed-integer linear programming model to optimize the trading interactions, considering the operational cost of the MG and the potential revenue for EV owners. The proposed approach can be used to formulate a trading mechanism among the grid, EVs, and MGs. The following are the key contributions of the study:

- An incentivized pricing scheme for EV owners is developed that encourages them to sell their stored energy back to the grid during peak load periods. This scheme not only incentivizes EV owners but also takes into account the potential financial strain on the grid.
- A multi-objective optimization model is developed to balance the two contradictory objectives: minimization of the MG cost and maximization of the EV owners' revenue. This model is designed to simultaneously address the needs of multiple entities.
- Monte Carlo simulations (MCSs) are performed to deal with uncertainty in EV parameters. By employing MCSs, this study accounts for real-world variability and complexities, ensuring that the developed model is both practical and reliable.
- Finally, a detailed analysis is conducted to analyze the impact of different weights assigned to the objectives and EV fleet size. This analysis recognizes that different stakeholders may prioritize objectives differently and that the fleet size may change over time. Through this analytical approach, it provides insights into how different factors influence the performance of the model.

The remainder of the paper is organized as follows. Section 2 outlines the system configuration, along with a discussion of the trading mechanism and the structure of trading prices, which includes the incentivized selling price. In Section 3, uncertain parameters associated with EVs are discussed, using MCS. The proposed optimization method is presented in Section 4. The simulation results and analysis of results are presented in Section 5. Section 6 analyzes the influence of different weight parameters and the effects of increasing the fleet size. Finally, the conclusion is presented in Section 7.

2. Proposed Trading Mechanism

2.1. System Configuration

The proposed system consists of a network of three entities: an MG, a parking lot for EVs, and the distribution system operator (DSO). The MG system consists of two diesel generators (DGs), a renewable distributed generation (RDG), a battery storage system (BESS), and the electric load of a commercial building. The proposed network framework is shown in Figure 1. Energy trading among different entities is carried out via the power link. However, the trading price information from the DSO, including incentivized selling price C_t^{ES} for EV owners, is communicated to the community energy management system (EMS)

via the communication link. Having the price information from DSO and considering the internal trading price signals between MG and EVs, EMS is responsible for performing optimization based on the given operational objectives.

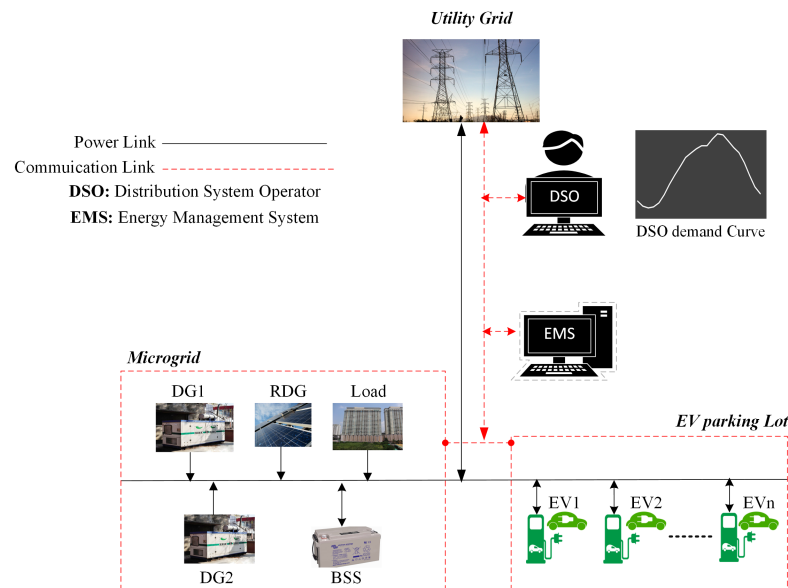


Figure 1. System configuration of the proposed network.

It should be noted that EVs in the parking lot can only be used during their parking periods. The usable window for EVs present in the parking lot is different for commercial and residential vicinities with reference to the time of arrival (t_a) and departure (t_d). In this study, a parking lot for a commercial area is considered, in which the arrival at the parking place is usually in the morning and departure is in the evening.

2.2. Pricing Structure

Energy trading among different entities is divided into two levels in this study, external and internal. For the external level, DSO is responsible for determining the trading prices for MG and EV owners at each interval. The trading prices consist of grid buy price (C_t^{GB}), grid sell price (C_t^{GS}), and incentivized selling price (C_t^{ES}). The incentivized selling price is offered to EV owners during peak demand intervals; the details are discussed in the subsequent sections. Contrarily, the internal market prices consist of the internal buy price (C_t^{IB}) and internal sell price (C_t^{IS}). These prices are determined such that they are in between C_t^{GB} and C_t^{GS} . This is to encourage internal trading while maximizing the profitability of internal trading entities.

2.3. Incentivized Selling Price for EV Owners

To overcome equipment overloading of DSO during peak load intervals and to encourage the adoption of V2G service among EV owners, an incentivized selling price (C_t^{ES}) framework is formulated in this study. The design of this pricing scheme must consider various factors to ensure that it remains within the boundaries of C_t^{GB} and C_t^{GS} , thereby preventing unnecessary financial strain on the DSO. Moreover, the C_t^{ES} should be adaptable and responsive to changes in demand, enabling dynamic adjustments that motivate EV owners to engage in V2G services while maintaining grid stability and efficiency.

In the proposed approach, we used a sigmoid function $S(z_t)$ to formulate C_t^{ES} . The sigmoid function has a smooth and continuous nature that ensures gradual changes [42]. This property ensures that small changes in the input lead to small changes in the output, providing a gradual transition. This helps avoid abrupt jumps that could lead to instability. Other traditionally used functions, like piecewise linear function, can create abrupt changes at the transition points between different segments. These discontinuities at the threshold

may not accurately reflect the changes in inputs, leading to unrealistic representations of the output. Thus, the sigmoid function provides more reliable modeling of C_t^{ES} in our energy trading context. It provides a smooth transition between C_t^{GB} and C_t^{GS} based on the demand of DSO. Mathematically, it can be represented as

$$S(z_t) = \frac{1}{1 + e^{-z_t}} \quad (1)$$

To facilitate scaling, demand is normalized and subjected to a sigmoid function. Then, grid price weights are computed through the application of the sigmoid function as shown in Equations (2) and (3):

$$\alpha_t = S(z_t) \cdot C_t^{GB} \quad (2)$$

$$\beta_t = 1 - S(z_t) \cdot C_t^{GS} \quad (3)$$

In Equations (2) and (3), the buy price weight (α_t) and sell price weight (β_t) are calculated by applying $S(z_t)$. It means that when the demand is high, α_t is closer to C_t^{GB} and the corresponding β_t will be low and vice versa:

$$C_t^{ES} = \alpha_t \cdot C_t^{GB} + \beta_t \cdot C_t^{GS} \quad (4)$$

After the calculation of weights, the C_t^{ES} is calculated as the weighted sum of C_t^{GB} and C_t^{GS} using Equation (4). Thus, the C_t^{ES} is adjusted based on the demand. The procedure for the calculation of C_t^{ES} is shown in Algorithm 1.

Algorithm 1: Calculation of incentivized selling price for EV owners

Input: $T = 24$, DSO demand profile, C_t^{GB} , C_t^{GS}

- 1 Define high demand intervals t_1 and t_2
- 2 Apply sigmoid to normalized DSO demand (1)
- 3 **for** $t < T$ **do**
- 4 **if** $t_1 \leq t \leq t_2$ **then**
- 5 Calculate the sigmoid weight for C_t^{GB} (2)
- 6 Calculate the weight for C_t^{GS} (3)
- 7 Compute C_t^{ES} as the weighted average of C_t^{GB} and C_t^{GS} , using respective weights (4)
- 8 **else**
- 9 Set C_t^{ES} equal to C_t^{GS}
- 10 Store the calculated C_t^{ES}
- 11 $t = t + 1$

Output: Values of incentivized price for EVs (C_t^{ES})

In this algorithm, we first initialize the time horizon $T = 24$ h, DSO demand profile, C_t^{GB} and C_t^{GS} . Then, we define the high-demand intervals from t_1 to t_2 . After the normalization of the DSO demand, the algorithm iterates through each hour of the day. During high-demand intervals, the sigmoid weight is calculated using Equations (2) and (3), then C_t^{ES} is calculated as a weighted sum using Equation (4). For non-peak intervals, the C_t^{ES} is assigned the same value as the C_t^{GS} .

2.4. Trading Mechanism

The trading mechanism consists of two market levels based on the pricing structure described previously. An overview of the trading mechanism is shown in Figure 2.

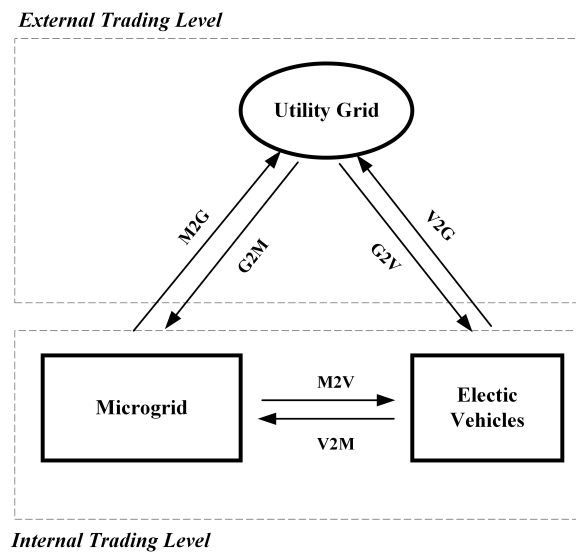


Figure 2. An overview of trading mechanism among different entities.

2.4.1. External Level

At the external level, both the MG and EVs can trade power with the utility grid. The MG can buy power from the utility grid (Grid-to-MG: G2M) at C_t^{GB} when local generation is insufficient, and it can sell excess power to the utility grid (MG-to-Grid: M2G) at C_t^{GS} . Similarly, EVs can also interact with the utility grid, buying power for charging (grid-to-EVs: G2V) at C_t^{GB} and selling the surplus stored energy at C_t^{ES} , through the V2G mechanism.

2.4.2. Internal Level

At the internal level, the MG and EVs can trade power with each other through (EVs-to-MG: V2M) and (MG-to-EVs: M2V) mechanisms. Both entities can buy power from each other at C_t^{IB} and sell their excess power at C_t^{IS} .

The bi-level trading between these three entities occurs simultaneously. The simultaneous bi-level trading mechanism enables a flexible response to varying the generation, load, and energy storage conditions. In addition, it provides an efficient solution for energy management in this networked system.

3. Electric Vehicles Parameters Calculation

There are several parameters related to EVs, which include uncertainty, such as arrival time t_a , departure time t_d , and the initial state of charge SOC^{ini} . These parameters play a crucial role in the assessment of the EV charging demand. The accurate consideration of these factors leads to the precise decision making and scheduling of the energy resources. To cope with these random parameters, Monte Carlo simulation (MCS) is used. The MCS method is a computational technique that employs random sampling to simulate and analyze complex systems. Based on the probability theory, this stochastic algorithm can accurately model real-world phenomena and physical experimental procedures [43]. The predictive accuracy largely depends on the quality of the historical data. However, this method effectively simulates random processes, apt for forecasting the unpredictable behaviors of EVs [44].

3.1. EV Arrival and Departure Times

Our model features a parking lot designated for commercial areas. In these types of parking lots, EVs typically arrive in the morning and leave in the evening. It is assumed that the arrival time t_a and departure time t_d follow a normal distribution, which can be represented mathematically as in Equations (5) and (6):

$$f(t_a) = \begin{cases} \frac{1}{\sqrt{2\pi\sigma_{t_a}}} \exp\left(-\frac{(t_a-\mu_{t_a})^2}{2\sigma_{t_a}^2}\right), & 0 < t_a \leq \mu_{t_a} + 12 \\ \frac{1}{\sqrt{2\pi\sigma_{t_a}}} \exp\left(-\frac{(t_a-24-\mu_{t_a})^2}{2\sigma_{t_a}^2}\right), & \mu_{t_a} + 12 < t_a \leq 24 \end{cases} \quad (5)$$

$$f(t_d) = \begin{cases} \frac{1}{\sqrt{2\pi\sigma_{t_d}}} \exp\left(-\frac{(t_d-\mu_{t_d})^2}{2\sigma_{t_d}^2}\right), & 0 < t_d \leq \mu_{t_d} - 12 \\ \frac{1}{\sqrt{2\pi\sigma_{t_d}}} \exp\left(-\frac{(t_d-24-\mu_{t_d})^2}{2\sigma_{t_d}^2}\right), & \mu_{t_d} + 12 < t_d \leq 24 \end{cases} \quad (6)$$

where μ_{t_a} and μ_{t_d} are the mean of the arrival and departure times, and σ_{t_a} and σ_{t_d} are the standard deviations, respectively. The data of the arrival and departure times of the vehicles are taken from [45], and the corresponding density functions are shown in Figure 3.

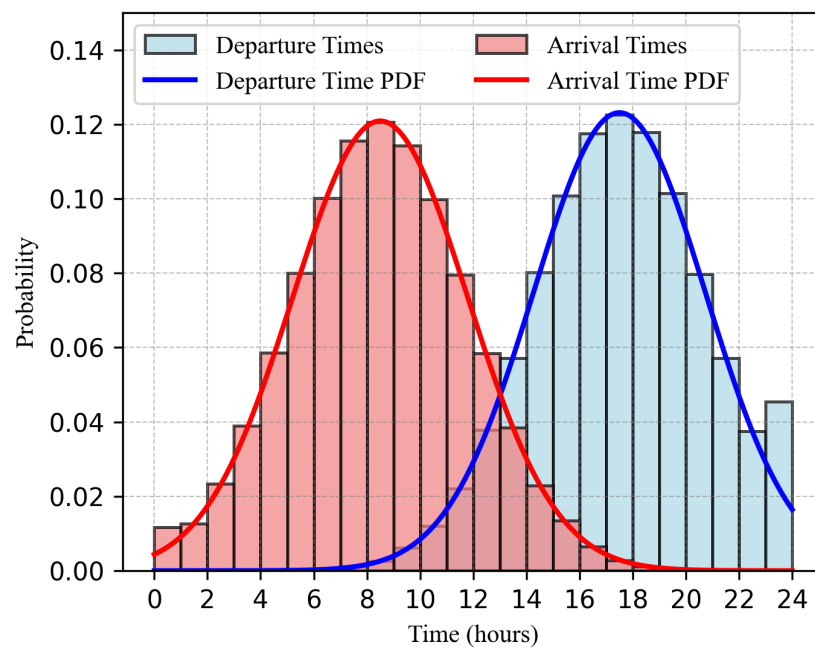


Figure 3. MCS results of arrival and departure times of EVs based on PDF of historical data.

3.2. Daily Mileage of EVs

The SOC^{ini} is influenced by the distance traveled by EVs before reaching the parking lot. The distance traveled by the vehicle to reach the parking lot is represented by d . It is assumed that the daily driving distance follows a log-normal distribution, which can be mathematically expressed as in Equation (7):

$$f(d) = \frac{1}{d \cdot \sigma_d \cdot \sqrt{2\pi}} \exp\left(-\frac{(\ln d - \mu_d)^2}{2\sigma_d^2}\right) \quad (7)$$

where μ_d represents the mean and σ_d represents the standard deviation of the driving distances. The daily driving mileage of vehicles is taken from [46], and only private vehicles are analyzed. The PDF of the daily driving distance is shown in Figure 4.

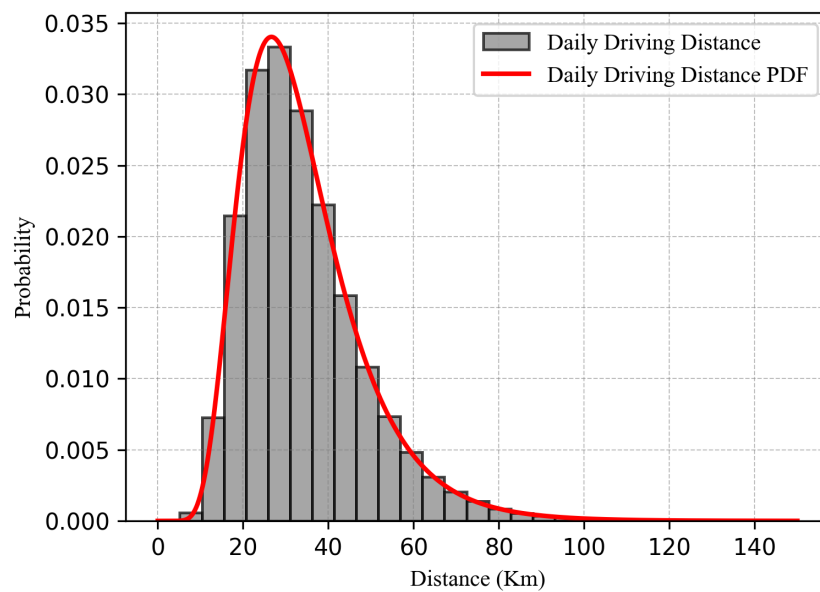


Figure 4. MCS results of daily driving distances of EVs based on PDF of historical data.

3.3. Monte Carlo-Based EV Parameter Estimation

Monte Carlo simulation comprises three steps: distribution determination, random number generation, and result analysis. In this study, MCS is used to estimate the randomness in the EV parameters based on the initial probability distribution. The following steps outline the process of extracting the probable driving distance and arrival/departure times for EVs:

- Initialize the dataset that includes N EVs. Initialize the PDF mean and standard deviation of the driving distance, arrival time and departure time of the EVs. Set the number of iterations.
- Generate random samples based on the log-normal distribution for the daily driving distance and normal distribution for arrival and departure times.
- Analyze the results and select random iteration from the collection of outcomes.

The histograms in Figure 3 represent the generated data using MCS according to the given PDFs. It can be seen from the results that most of the EV owners usually arrive at the parking lot at approximately 9 a.m. and depart at 6 p.m. These results align with the traveling behavior of daily commuters. Similarly, Figure 4 represents the histogram of the daily mileage of EVs, where most of the vehicles travel less than 80 km.

3.4. EV SOC Computation

The SOC^{ini} refers to the remaining battery capacity of an EV when it arrives at the parking lot. It is influenced by the SOC at the time of leaving home SOC^{start} and the distance traveled before reaching the parking lot d :

$$SOC^{ini} = SOC^{start} - \frac{d}{D} \quad (8)$$

In Equation (8), D represents the maximum driving range of the EV, and d represents the daily driving distance of the EV that is extracted from MCS. Finally, by putting these values in Equation (8), SOC^{ini} can be determined.

4. Problem Formulation

The problem is formulated as a multiobjective optimization problem considering two main objectives. The first objective is to minimize the cost for the MG, and the second objective is to maximize the revenue for EV owners through energy trading.

4.1. Cost Minimization Function for Microgrid

The aim of the MG objective function is to minimize its operational cost. The objective function of MG shown in Equation (9) consists of the costs incurred by buying the energy to fulfill its local demand and the revenue ($P_{t,n}^{M2V}$, P_t^{M2G}) generated by selling its surplus energy. The cost component consists of three terms: the first term is associated with the cost of DG ($C_{k,t}^{DG}$), the second term corresponds to the cost of purchasing energy from the grid (P_t^{G2M}), and the third term represents the cost of purchasing energy from EVs ($P_{t,n}^{V2M}$). On the revenue side, the first term signifies the income generated from selling energy to the grid (P_t^{M2G}), while the second term captures the revenue obtained from supplying energy to EV owners ($P_{t,n}^{M2V}$):

$$f_1(\mathbf{x}) = \min \sum_{t=1}^T \left(\sum_{k=1}^K C_{k,t}^{DG} \cdot P_{k,t}^{DG} \right) + C_t^{GB} \cdot P_t^{G2M} + \left(\sum_{n=1}^N C_t^{IB} \cdot P_{t,n}^{V2M} - C_t^{IS} \cdot P_{t,n}^{M2V} \right) - C_t^{GS} \cdot P_t^{M2G} \quad (9)$$

4.2. Revenue Maximization Function for EV Owners

The objective function for EV owners is to maximize their revenue represented in Equation (10). The first two terms represent the revenue generated by selling stored energy to other entities ($P_{n,t}^{V2G}$, $P_{n,t}^{V2M}$) and the incurred cost is represented by the next two terms, i.e., buying energy from other entities ($P_{n,t}^{G2V}$, $P_{n,t}^{M2V}$):

$$f_2(\mathbf{x}) = \max \sum_{t=1}^T \sum_{n=1}^N C_t^{ES} \cdot P_{n,t}^{V2G} + C_t^{IS} \cdot P_{n,t}^{V2M} - C_t^{GB} \cdot P_{n,t}^{G2V} - C_t^{IB} \cdot P_{n,t}^{M2V} \quad (10)$$

4.3. Constraints

The above-given objective function is subjected to several constraints, which are discussed in the following subsections.

4.3.1. Distributed Generators (DG)

Equation (11) represents the operating bounds of DG, where P_{min}^{DG} represents the minimum operation value and P_{max}^{DG} represents the maximum operating value of DG:

$$P_{min}^{DG} \leq P_{k,t}^{DG} \leq P_{max}^{DG} \quad (11)$$

4.3.2. BESS Charging and Discharging

Equations (12)–(15) represent the constraints of BESS related to charging, discharging, and SOC estimation (SOC_t^B) of the BESS:

$$SOC_{min}^B \leq SOC_t^B \leq SOC_{max}^B \quad (12)$$

$$0 \leq P_t^{B+} \leq \frac{P_{cap}^B \cdot (1 - SOC_{t-1}^B)}{\eta^{B+}} \quad (13)$$

$$0 \leq P_t^{B-} \leq P_{cap}^B \cdot (SOC_{t-1}^B) \cdot \eta^{B-} \quad (14)$$

$$SOC_t^B = SOC_{t-1}^B + \frac{\eta^{B+} \cdot P_t^{B+} - \frac{1}{\eta^{B-}} (P_t^{B-})}{P_{cap}^B} \quad (15)$$

The charging (η^{B+}) and discharging (η^{B-}) efficiencies of the BESS are considered, following the approach used in [47]. During the discharging periods, the BESS functions as an energy source, while it acts as a load during the charging periods. Equation (12) ensures that SOC_t^B remains within a specified range at each time interval. Moreover, to ensure that BESS charging (P_t^{B+}) and discharging (P_t^{B-}) are within the maximum capacity (P_{cap}^B)

limit of the BESS, Equations (13) and (14) are formulated. These constraints prevent the overcharging and deep discharging of BESS. SOC_t^B is updated using Equation (15).

4.3.3. EV Charging and Discharging

The charging and discharging mechanisms of EVs is similar to that of BESS, with some additional modifications to account for their specific characteristics and requirements. The charging and discharging constraints of EVs are formulated as Equations (16)–(20):

$$SOC_{min}^{EV} \leq SOC_{n,t}^{EV} \leq SOC_{max}^{EV} \quad (16)$$

$$0 \leq (P_{n,t}^{M2V} + P_{n,t}^{G2V}) \leq \frac{P_{cap}^{EV} \cdot (1 - SOC_{n,t-1}^{EV})}{\eta^{EV+}} \quad (17)$$

$$0 \leq (P_{n,t}^{V2M} + P_{n,t}^{V2G}) \leq P_{cap}^{EV} \cdot (SOC_{n,t-1}^{EV}) \cdot \eta^{EV-} \quad (18)$$

$$SOC_{n,t}^{EV} = SOC_{n,t-1}^{EV} + \frac{\eta^{EV+} \cdot (P_{v,t}^{M2V} + P_{v,t}^{G2V}) - \frac{1}{\eta^{EV-}} (P_{n,t}^{V2M} + P_{n,t}^{V2G})}{P_{cap}^{EV}} \quad (19)$$

$$SOC_{n,t,d}^{EV} \geq SOC_{min}^{EV} \quad (20)$$

Similar to BESS, the charging and discharging efficiencies of EVs are considered. Equation (16) ensures that the SOC of EVs ($SOC_{n,t}^{EV}$) remains within a specified range. EVs can gain energy from the MG ($P_{n,t}^{M2V}$) and grid ($P_{n,t}^{G2V}$) for charging. Similarly, EVs can be discharged to supply energy to the MG ($P_{n,t}^{V2M}$) and the grid ($P_{n,t}^{V2G}$) when needed. Equations (17) and (18) are designed to ensure that EVs charge and discharge within their bounds while trading power with MG and the grid. Equation (19) is formulated to update ($SOC_{n,t}^{EV}$) of EVs. Furthermore, Equation (20) is formulated to guarantee that the SOC of the EVs at the time of departure ($SOC_{n,t,d}^{EV}$) meets the specific requirements of the EV owners, ensuring their needs are satisfied.

4.3.4. Power Balance

The power balance of the MG is illustrated in Equation (21). It indicates that power generation must be equal to the power consumption for each time interval:

$$P_t^{G2M} + P_t^{RDG} + \sum_{k=1}^K P_{k,t}^{DG} + \sum_{n=1}^N (P_{n,t}^{V2M} - P_{n,t}^{M2V}) + P_t^{B-} - P_t^{B+} - P_t^{M2G} = P_t^{Load} \quad (21)$$

It ensures that MG local demand P_t^{Load} can be met by generation from DGs, RDG, BESS charging/discharging, and energy exchanges with the grid and EVs.

The formulated problem consist of various types of decision variables and constraints; the decision variables represented in Equations (9) and (10) are continuous and non-negative. They typically represent the power flow between the MG, N number of EVs, and the grid, as well as the K number of DGs power for a total time step of T. The constraints given in Equations (11)–(21) are categorized into bounding, equality, and inequality constraints:

- The bounding constraints, defined in Equations (11)–(14) and (16)–(18), encompass the operating bounds of the K number of DGs, BESS, and N number of EVs for charging and discharging for a total time step of T.
- The inequality constraints are specified in Equation (20) to ensure that the SOC of the N number of EVs meets specific requirements on the departure for a total time step of T.

- Lastly, the equality constraints are presented in Equations (15), (19) and (21), representing the SOC estimation of BESS and N number of EVs, as well as the power balance in the MG system for a total time step of T.

Overall the total number of the decision variables and constraints depends on the values of K, N and T, representing the total number of DGs, EVs and time step, respectively.

4.4. Optimization Method

The scalarization or weighted sum method is used to solve this multi-objective optimization problem. In this method, weights are assigned to each objective as shown in Equation (22) [48], and then the weighted sum is optimized:

$$\min f(x) = \min \sum_{i=1}^n w_i \cdot f_i(x) \quad (22)$$

In this formulation, $f(x)$ represents the overall objective function, while w_i denotes the weights assigned to the objectives such that the sum of all the weights is equal to 1 as shown in Equation (23):

$$\sum_{i=1}^n w_i = 1 \quad (23)$$

The weighted sum method simplifies complex problem solving with its straightforward approach, outperforming multi-step alternatives. It excels in handling programming, software use, computational complexity, and preference information as noted in [49]. The weighted sum can be mathematically represented as

$$\min f(x) = \min[w_1 \cdot f_1(x) - w_2 \cdot f_2(x)] \quad (24)$$

$$w_2 = 1 - w_1 \quad (25)$$

where the selection of w_1 and w_2 is in the range [0,1].

By using this approach, multi-objective problems can be changed into a single objective problem. As a result, the optimal solutions of single-objective problems are like Pareto optimal solutions of multi-objective problems.

5. Numerical Simulation

The performance of the proposed optimization method is tested for a scheduling horizon of 24 h with a time interval of 1 h. This formulated multi-objective optimization problem is based on mixed-integer linear programming (MILP) and is implemented in Visual Studio 2019 with the integration of IBM CPLEX 22.1.0 [50]. The simulations are conducted on a Core i5 PC equipped with 8 GB of RAM.

5.1. Input Parameters

5.1.1. Trading Prices

Trading prices for MG and EVs are composed of grid prices and internal prices. Both grid and internal price signals are the same as in [38], as shown in Figure 5. The C_t^{IS} at the DSO level depends on three factors: C_t^{GB} , C_t^{GS} , and DSO demand. The DSO demand data are derived from [51] and are shown in Figure 6.

The C_t^{ES} is equal to C_t^{GS} at non-peak demand intervals and higher than C_t^{GS} during the peak demand periods. In this analysis, peak demand intervals for the DSO are assumed to occur when the demand exceeds 6500 kW, specifically within 10–19 intervals. Algorithm 1 is employed to calculate the C_t^{ES} . The results are shown in Figure 7.

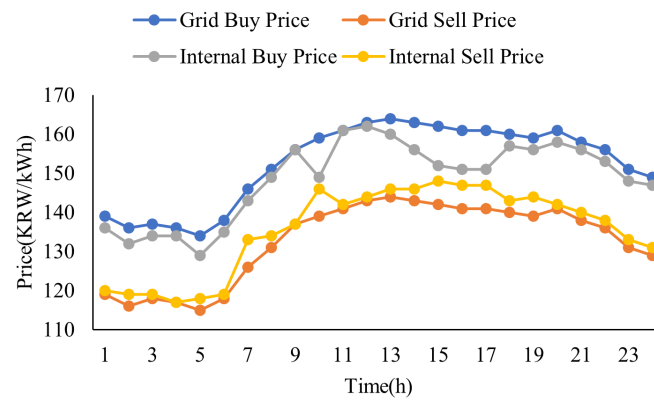


Figure 5. External and internal trading prices.

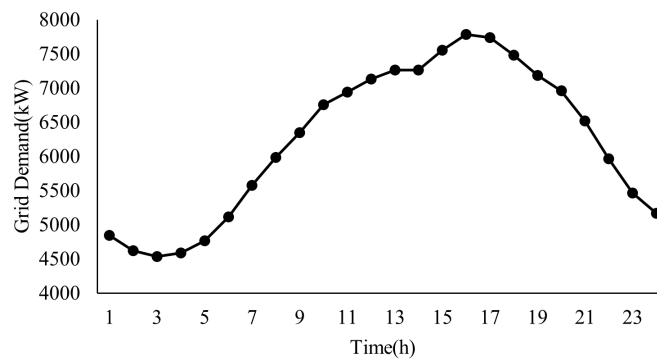


Figure 6. Utility grid demand data of 24 h at DSO.

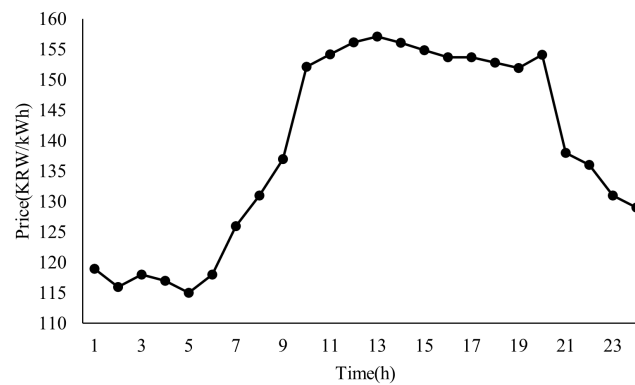


Figure 7. Calculated incentivized selling price data for EV owners.

5.1.2. EV Parameters

In this study, a dataset of 20 EVs is selected from [52]. The dataset includes EV parameters, such as EV ID, name, capacity and maximum driving range, denoted by D . An overview of these parameters is shown in Table 1.

In addition, other EV parameters, such as arrival time, departure time, and the initial SOC are essential for evaluating EV performance. In this study, MCS was employed to estimate the daily driving distance, arrival, and departure times, as depicted in Figures 3 and 4. These uncertain parameters for 20 EVs were randomly selected from MCS by using a seed value of 25 to ensure reproducibility, displayed in Table 2. The random selection of these parameters based on the given PDF provides a glimpse into potential real-world scenarios and facilitates a more realistic representation.

To compute the SOC^{ini} of EVs, (8) is utilized. The SOC of EVs when they begin their trip to reach a parking lot SOC^{start} is randomly chosen between 60 and 90 percent as shown in Table 2, with a seed value of 25. This range indicates that it satisfies the daily driving needs of EV owners. In a similar fashion, 20 EVs were chosen from the MCS for daily driving distances (d), as illustrated in Figure 4, using a seed value of 25. Using these data, the SOC^{ini} was calculated, presented in Table 2. The charging and discharging efficiencies of EV batteries are considered to be 95% for all the EVs.

Table 1. Parameters of selected EVs for simulations.

EV-ID	Name	Capacity (kWh)	Range (km)
1	Hyundai IONIQ 6 Standard Range	54	360
2	Kia EV6 GT	74	370
3	Mini Cooper SE	28.9	180
4	Tesla Model 3	57.5	380
5	BMW iX3	74	385
6	Ford Mustang Mach-E GT	91	425
7	Honda e Advance	28.5	170
8	Volkswagen ID.3 Pro	58	350
9	Lexus UX 300e	45	235
10	Porsche Taycan Turbo S	83.7	400
11	Nissan Leaf	39	235
12	Kia e-Soul 39.2 kWh	39.2	230
13	Polestar 2 Long Range Performance	78	410
14	Dacia Spring Electric 45	25	165
15	Jeep Avenger Electric	50.8	300
16	Mercedes EQE 350+	90.6	525
17	Audi e-tron GT RS	85	405
18	Toyota Proace City Verso Electric L1	46.3	210
19	Genesis GV70 Electrified Sport	74	350
20	Renault Twingo Electric	21.3	130

Table 2. Arrival/departure time and SOC of EVs.

EV-ID	Arrival Time (h)	Departure Time (h)	Starting SOC (%)	Initial SOC (%)
1	9	17	71	52
2	11	17	88	71
3	6	24	85	60
4	11	17	66	53
5	13	18	86	78
6	1	19	79	66
7	8	21	61	33
8	8	13	89	84
9	8	17	68	48
10	12	22	69	57
11	9	24	73	49
12	4	19	78	44
13	10	12	64	51
14	10	21	81	59
15	10	16	85	72
16	6	18	75	66
17	14	17	84	72
18	12	18	79	70
19	8	20	85	74
20	11	16	65	24

5.1.3. Microgrid Parameters

The local load profile of the MG is a scaled version of [53], and is shown in Figure 8. The MG has two DGs: DG1 with a 100 kW capacity at a cost of 80 KRW/kWh, and DG2 with a 150 kW capacity at a cost of 100 KRW/kWh. The BESS capacity is 100 kWh with 95% charging and discharging efficiency. Moreover, the initial state of charge of BESS is considered 20%. The output of RDG in MG is a scaled version of [54] and is shown in Figure 9.

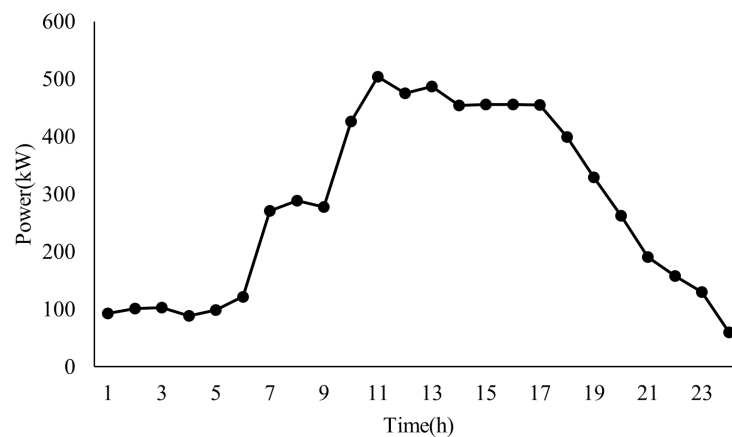


Figure 8. Load profile of microgrid.

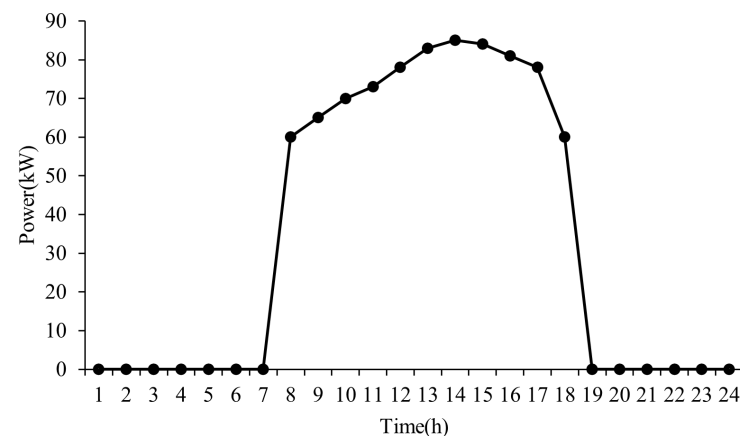


Figure 9. Renewable distributed generation (RDG) output power profile.

5.2. Simulation Results

In this section, two cases are analyzed, each reflecting different weight parameters for the cost minimization function of MG and the revenue maximization function of EVs. In the first case, a higher weight is assigned to the MG cost minimization function compared to the EV owners' profit. In the second case, more weight is assigned to the revenue of EVs as compared to the MG cost. RDGs are photovoltaic systems that are available and can contribute to the energy supply during daylight hours. DGs are utilized throughout the day. BESS is charged during periods of low demand and discharged during peak times. Some variations are observed in energy trading among EVs, grid and MG due to different weights.

5.2.1. Case 1

In this scenario, a weight of 0.7 is assigned to the cost function of the MG, while a corresponding weight of 0.3 is assigned to the revenue of the EVs. Figure 10a presents the optimal results from the MG perspective. Energy trading from the MG to the grid occurs

during intervals 1–6, 9, and 21–24. Similarly, energy transfer from MG to EVs occurs during intervals 5, 6, 8, and 22–24, as the local generation cost is lower than the C_t^{GS} and C_t^{IS} ; also, the local demand of the MG is less than the local generation. The MG receives energy from EVs during the intervals 15–17, as C_t^{IS} is lesser as compared to C_t^{GB} .

Figure 10b illustrates the optimal energy trading with the EVs perspective. Upon arrival, EVs tend to purchase energy from the MG during intervals 5, 6, and 8 and from the grid during intervals 7–9 to charge to the targeted SOC level. Before departure, EVs buy power from the grid and MG during intervals 19 and 21–24 to meet their energy requirements. As in this case, the MG cost function is prioritized so the model is operating such that it tends to be more focused on the cost minimization of MG. That is why more energy is traded from EV to MG at peak hours because it is more economical for MG to buy from EVs instead of buying from the grid.

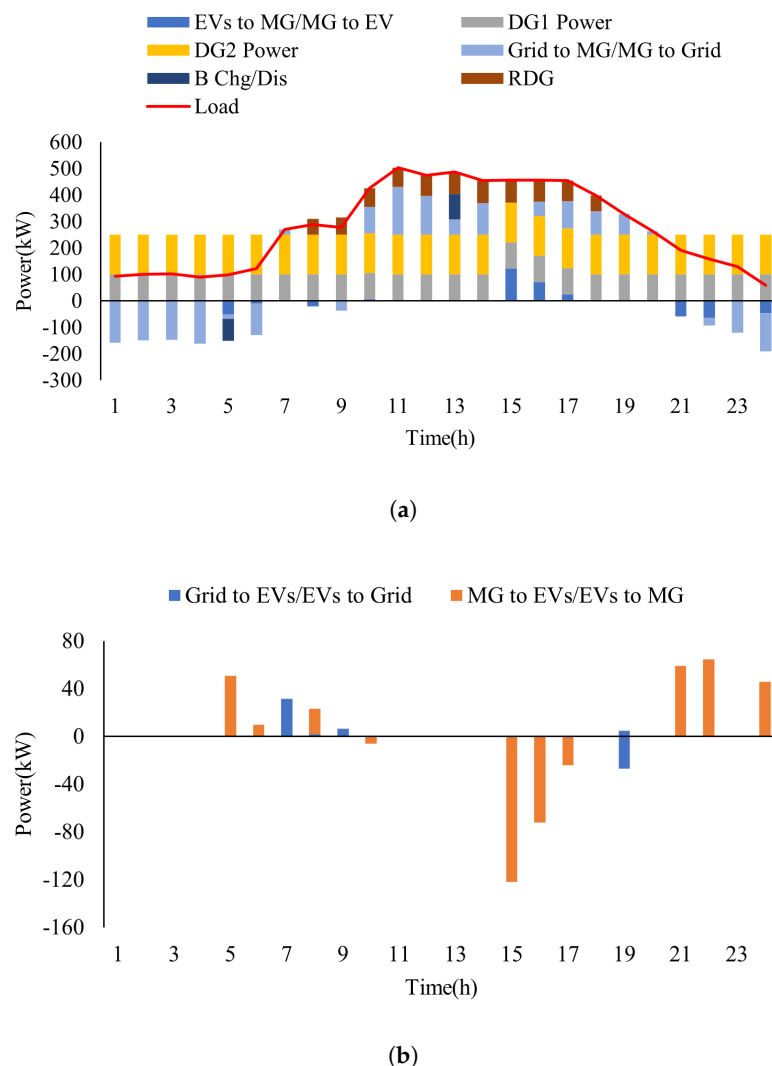
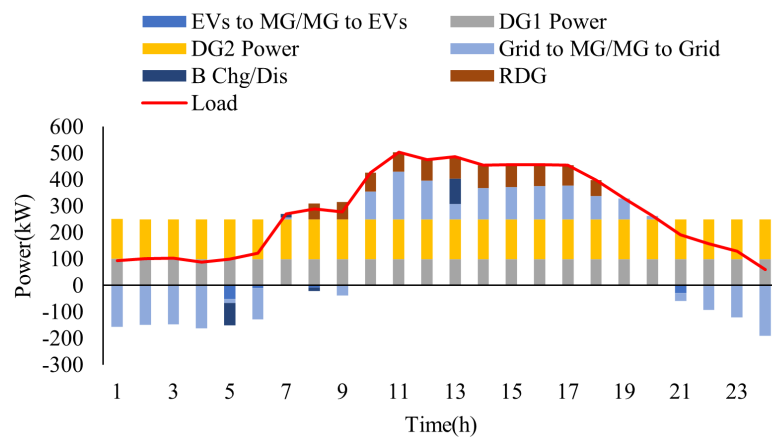


Figure 10. Optimal results for microgrid and EV owners for case 1: (a) microgrid perspective; (b) EV owner perspective.

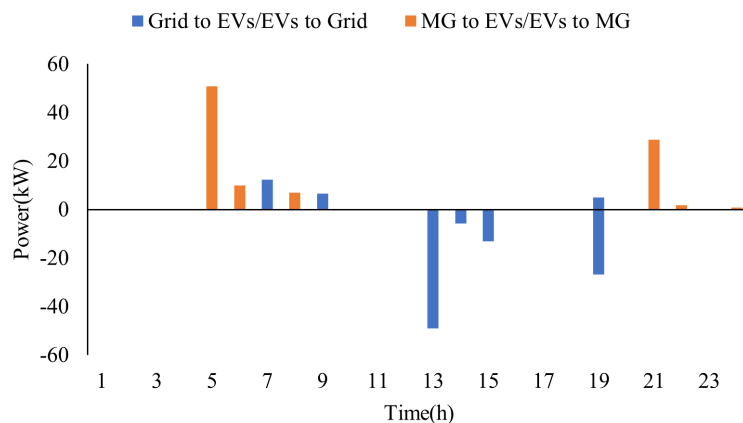
5.2.2. Case 2

In this case, a weight of 0.3 is assigned to the cost function of the MG, while the corresponding weight for EVs is set at 0.7. Figure 11a,b present the optimal operation and energy trading results. Energy trading from the MG to the grid takes place during intervals 1–6, 9, and 21–24. Similarly, energy transfer from MG to EV occurs during intervals 5, 6 and 8, as the local generation cost of the MG is lower than C_t^{GS} and C_t^{IS} . Energy trading from the grid to EVs occurs upon arrival at intervals 7–9 and during interval 19 to meet the

energy requirements for departure. Energy trading from EVs to the grid takes place during intervals 13–15 and 19, specifically during peak intervals of the grid demand from 13 to 15, as high C_t^{ES} is offered to EV owners during these periods. Notably, at interval 13, the maximum number of EV owners tend to sell their energy, as the C_t^{ES} offered to them is the highest compared to other intervals. In this case, the revenue function of EV is prioritized, so more EVs are engaged in trading with the grid because C_t^{ES} at peak intervals is greater than the C_t^{IS} .



(a)



(b)

Figure 11. Optimal results for microgrid and EV owners for case 2: (a) microgrid perspective; (b) EV owner perspective.

These results demonstrate the impact of varying weight allocations on the energy-trading patterns among the MG, EVs, and the grid. The energy trading dynamics vary depending on the prioritization of the objectives. When the MG cost function is prioritized, it tends to buy more energy from the EVs, as C_t^{IB} is less compared to C_t^{GB} . Conversely, when the EVs revenue function is given more weightage, the energy trading from EVs to the grid increases, especially during peak intervals when high C_t^{ES} is offered. The findings demonstrate the trade-offs between the objectives of the MG and EV owners, optimizing their operations in accordance with their respective preferences.

6. Discussion and Analysis

6.1. Impact of Weight Parameters

In this section, we examine five different cases through simulation, focusing on the total amount of energy traded within a 24 h span as detailed in Table 3. For the first

two cases, the weight assigned to the cost minimization of the MG, represented by w_1 , is set higher compared to the weight of the EVs profit, denoted by w_2 . When the MG cost minimization is emphasized, the MG tends to trade more energy with the EVs than with the grid, thereby minimizing its costs. This is because the value of C_t^{IB} is lower as compared to C_t^{GB} , allowing the MG to purchase energy at a more affordable rate. Moreover, the C_t^{IS} is higher than C_t^{GS} , enabling the MG to sell its energy at a higher price. In the third case, equal weights are assigned to the MG cost minimization function and the EVs profit maximization functions. During periods of peak demand, the MG acquires power from the EVs to reduce its costs. Simultaneously, EVs sell power to the grid when C_t^{ES} is at its maximum, thereby maximizing their revenue. The last two scenarios are characterized by assigning more weight to the EVs profit. This focus on maximizing the EVs profit leads to less energy trading with MG as compared to the grid because during peak intervals, C_t^{ES} is higher compared to C_t^{IS} .

Figure 12 provides a clear depiction of the cost trends both for the EVs and the MG across five different cases. In the case of MG, an increasing trend in the total operation cost is observed from cases 1 to 5. Contrarily, a declining cost trend can be seen for EVs as we move from case 1 to case 5. The trends suggest a trade-off between the cost incurred by the EVs and the MG. Lower EV costs correspond with higher MG costs and vice versa. This indicates the varying balance between cost minimization and profit maximization in each case, influenced by the different weights assigned to each entity’s objectives.

Table 3. Energy trading with different weights.

Cases	Weights		Total Amount of Energy Traded (kWh)					
	w_1	$w_2 = 1 - w_1$	M2V	V2M	M2G	G2M	G2V	V2G
1	0.9	0.1	279	685	1049	503	513	14
2	0.7	0.3	251	224	1077	964	45	27
3	0.5	0.5	99	62	1214	1113	24	33
4	0.3	0.7	99	0	1215	1175	24	95
5	0.1	0.9	111	0	1192	1167	12	95

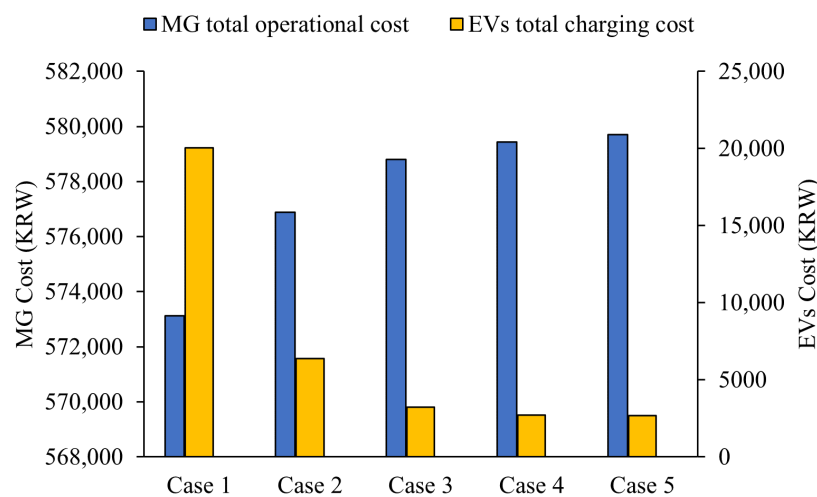


Figure 12. Total operational cost of microgrid and EVs.

Electric Vehicle Energy Trading Reference Indices

In this section, reference indices (I_x^{V2G}, I_x^{V2M}) are formulated for each case relative to case 3, in which equal weights are assigned to both objectives. These indices represent the relative change in energy trading from EVs to the grid and MG, taking into account variations in the weight parameters. The formulation is detailed in Equations (26) and (27), where ($E_{ref}^{V2G}, E_{ref}^{V2M}$) are the total amount of energy traded from EVs to the grid and MG

in the reference case, and (E_x^{V2G}, E_x^{V2M}) are the total amount of energy traded for cases referenced from case 3:

$$I_x^{V2G} = \frac{E_{\text{ref}}^{V2G} - E_x^{V2G}}{E_{\text{ref}}^{V2G}} \quad (26)$$

$$I_x^{V2M} = \frac{E_{\text{ref}}^{V2M} - E_x^{V2M}}{E_{\text{ref}}^{V2M}} \quad (27)$$

Figure 13 illustrates the variations in energy trading across different indices. In cases 1 and 2, the amount of energy trading from EVs to the grid is reduced, while trading to MG is increased with respect to reference case as represented by index 1 and 2. This occurs because the MG objective is prioritized, and C_t^{IB} is more favorable compared to the C_t^{GB} , prompting MG to buy more energy from EVs as compared to the reference case.

Conversely, in cases 4 and 5, the EV owner objective is prioritized, resulting in greater amount of energy trading with the grid rather than MG with respect to reference case, as represented by index 3 and 4. This trend emerges due to the grid's higher C_t^{ES} compared to the C_t^{IS} . In an effort to maximize revenue, EV owners are consequently more inclined to sell their energy to the grid as compared to the reference case.

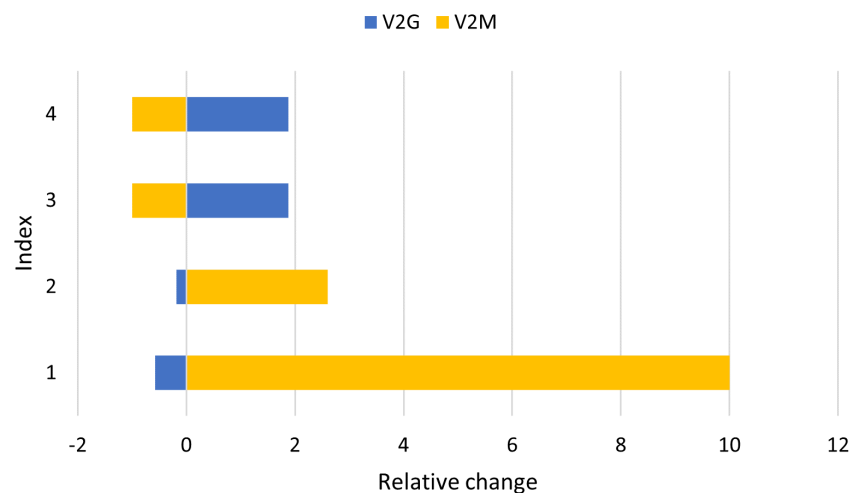


Figure 13. Energy-trading dynamics from EVs: case 3 reference.

6.2. Impact of Increase in Fleet Size

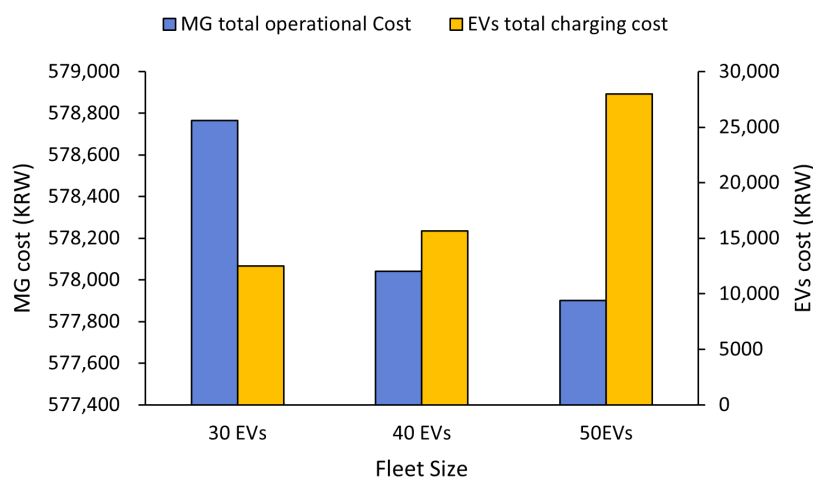
This section examines the influence on operational costs and the volume of energy exchanged as the fleet size expands. In this section, equal weights of 0.5 are designated for both the MG and EVs. By increasing the fleet size, we analyze the impact on the total amount of energy traded between these entities and the overall operational cost for the MG and charging cost for EVs.

Table 4 displays the cumulative quantity of energy traded between these entities based on the fleet size. It can be observed that as the fleet size increases, the energy interchange between the MG and EVs increases, while energy trading between MG and grid decreases. This is because the value of C_t^{IB} is lower than the C_t^{GB} , allowing each entity to procure energy at a reduced rate. Moreover, the value of C_t^{IS} is higher than the C_t^{GS} , which enables these entities to sell their power at higher rates. Additionally, the energy exchange between EVs and the grid increases due to an increase in the fleet size. With increases in the fleet size, the charging demand of EVs rises, and in the case of EV-to-grid interaction, an increasing number of EVs trade power with the grid during peak demand, as the C_t^{ES} surpasses both the C_t^{IS} and C_t^{GS} .

Table 4. Impact of increased fleet size on energy trading.

Fleet Size	Total Amount of Energy Traded (kWh)					
	M2V	V2M	M2G	G2M	G2V	V2G
30 EVs	119	62	1208	1126	64	33
40 EVs	173	122	1156	1066	100	37
50 EVs	252	122	1076	1066	145	72

Figure 14 shows the effect on costs associated with an increase in the EV fleet size. It is apparent from the figure that the cost of MG is lowered with an increase in the fleet size, while the charging cost for EVs increases. The MG cost reduces because, with a higher number of EVs, more EVs can function as an energy storage system at a lower cost. Furthermore, it also presents an opportunity for MG to trade energy at a higher price compared to the grid.

**Figure 14.** Impact of increase in fleet size.

The increase in EV fleet size has a significant impact on the energy-trading patterns and the operational cost of MG. It enhances energy exchanges within the MG and EVs while reducing grid dependency due to favorable internal pricing. Simultaneously, EVs serve as economical energy storage systems, providing a valuable energy-trading opportunity for MG. As the fleet size expands, the charging cost for EVs increases, but these vehicles also play a crucial role in supporting the grid at peak demand periods due to the higher incentivized selling price. Hence, strategic EV fleet management, coupled with internal energy trading, can not only optimize the operational cost of MG but also minimize grid dependency and reduce the peak load.

7. Conclusions

An incentive mechanism is proposed in this study to encourage EV owners to sell their energy to the grid during high-demand intervals to overcome the equipment overloading of distribution systems. Internal trading prices are also considered to maximize the participation and profitability of MG and EVs. Furthermore, to address the uncertainties in EV parameters, Monte Carlo simulations are used. The findings reveal that prioritizing the cost minimization of the MG leads to increased energy exchange between MG and EV, consequently lowering the operational cost of the MG. Conversely, when the profit of EV owners is prioritized, energy trading with the grid escalates, particularly during peak demand periods when the grid offers a higher selling price. Results showed that as the fleet size increases, the operational cost of MG decreases due to an increase in the energy transactions between MG and EVs. At the same time, though EVs face higher charging

costs owing to increased charging demand, they effectively function as economical energy storage systems, supporting the grid during peak demand periods.

Future studies can be conducted based on this research to explore the impact of different market policies, pricing mechanisms, and grid infrastructure on these trade-offs. This could assist the decision making of MG operators, EV owners and policymakers. In addition, a single MG is considered in this study but the potential for expansion to a multi-microgrid system exists. Such expansion could lead to the creation of a new kind of energy market and business model for EVs and MGs. Furthermore, the current model, which is designed with two objectives and does not consider power flow constraints, could be further refined. By incorporating multiple objectives and including power flow constraints, as in studies [55,56], the model could provide a more realistic and comprehensive approach to energy management.

Author Contributions: M.A.K.: conceptualization and writing—original draft preparation, A.H.: editing and analyzed the data, W.-G.L.: writing—review and editing H.-M.K.: validation and supervision. All authors have read and agreed to the published version of the manuscript.

Funding: This research received no external funding.

Data Availability Statement: Data availability not applicable.

Conflicts of Interest: The authors declare no conflict of interest.

Nomenclature

The following abbreviations are used in this manuscript:

Indices

t	Index for time interval, from 1 to T
n	Index for EV number, from 1 to N
k	Index for DG number, from 1 to K
x	index for the case number

Variables and Constants

z_t	Normalized DSO demand at time interval t
α_t, β_t	Weight of grid buy and sell price at time interval t
t_a, t_d	Arrival and departure time of EVs
t_1, t_2	Starting and ending time of high demand interval
$\sigma_{t_a}, \sigma_{t_d}$	Standard deviation of arrival and departure time of EVs
σ_d	Standard deviation of daily driving distances
μ_{t_a}, μ_{t_d}	Mean of arrival and departure time of EVs
μ_d	Mean of daily driving distances
η^{B+}, η^{B-}	Charging and discharging efficiency of BESS
η^{EV+}, η^{EV-}	Charging discharging efficiency of EVs
C_t^{GB}, C_t^{GS}	Price of buying and selling energy from the grid at t
C_t^{ES}	Incentivized selling price for EV owners at t
C_t^{IB}, C_t^{IS}	Price of buying and selling energy for EV and MG at t
$C_{k,t}^{DG}$	Cost of generating power from k^{th} DG at t
d	Daily driving distance of EVs
D	maximum driving range of EVs
SOC^{start}	State of charge of EVs at the start of the trip
SOC^{ini}	State of charge of EVs upon arrival at the parking lot
SOC_{n,t_d}^{EV}	State of charge of n^{th} EV at t_d
SOC_t^B	State of charge of BESS at t
$SOC_{n,t}^{EV}$	State of charge of n^{th} EV at t
$E_{ref}^{V2G}, E_{ref}^{V2M}$	Total amount of energy traded from EVs to the grid and MG for reference case
E_x^{V2G}, E_x^{V2M}	Total amount of energy traded from EVs to the grid and MG for case x
I_x^{V2G}, I_x^{V2M}	Reference indices for case x
P_{cap}^B, P_{cap}^{EVn}	Capacity of BESS and n^{th} EV
SOC_{min}^B, SOC_{max}^B	Minimum and maximum level of SOC for BESS

$SOC_{min}^{EV}, SOC_{max}^{EV}$	Minimum and maximum level of SOC for EV
P_t^{B+}, P_t^{B-}	Amount of power charged and discharged from BESS at t
$P_t^{G2M}, P_{n,t}^{G2V}$	Amount of power sent from grid to MG and n^{th} EV at t
$P_{n,t}^{M2G}, P_{n,t}^{M2V}$	Amount of power sent from MG to the grid and n^{th} EV at t
$P_{n,t}^{V2M}, P_{n,t}^{V2G}$	Amount of power sent from n^{th} EV to MG and the grid at t
P_t^{RDG}	Amount of power generated by RDG at t
$P_{k,t}^{DG}$	Amount of power generated by k^{th} DG at t
P_t^{Load}	MG Load at t

References

- Sedaghati, R.; Shakarami, M.R. A Novel Control Strategy and Power Management of Hybrid PV/FC/SC/Battery Renewable Power System-Based Grid-Connected Microgrid. *Sustain. Cities Soc.* **2019**, *44*, 830–843. [CrossRef]
- Dafnomilis, I.; den Elzen, M.; van Vuuren, D.P. Achieving Net-zero Emissions Targets: An Analysis of Long-term Scenarios Using an Integrated Assessment Model. *Ann. N. Y. Acad. Sci.* **2023**, *1522*, 98–108. [CrossRef]
- Ritchie, H. Cars, Planes, Trains: Where Do CO₂ Emissions from Transport Come from? *Our World in Data*. 2020. Available online: <https://ourworldindata.org/co2-emissions-from-transport> (accessed on 23 May 2023).
- Mckerracher, C. EVO Report 2022. 2023. Available online: <https://about.bnef.com/electric-vehicle-outlook/> (accessed on 17 May 2023).
- Ma, S.-C.; Xu, J.-H.; Fan, Y. Willingness to Pay and Preferences for Alternative Incentives to EV Purchase Subsidies: An Empirical Study in China. *Energy Econ.* **2019**, *81*, 197–215. [CrossRef]
- IEA. Global EV Outlook 2021. Available online: <https://www.iea.org/reports/global-ev-outlook-2021> (accessed on 23 May 2023).
- Muratori, M. Impact of Uncoordinated Plug-in Electric Vehicle Charging on Residential Power Demand. *Nat. Energy* **2018**, *3*, 193–201. [CrossRef]
- Kempton, W.; Letendre, S.E. Electric Vehicles as a New Power Source for Electric Utilities. *Transp. Res. Part D Transp. Environ.* **1997**, *2*, 157–175. [CrossRef]
- Sovacool, B.; Noel, L.; Axsen, J.; Kempton, W. The Neglected Social Dimensions to a Vehicle-to-Grid (V2G) Transition: A Critical and Systematic Review. *Environ. Res. Lett.* **2018**, *13*, 013001. [CrossRef]
- Kempton, W.; Tomić, J. Vehicle-to-Grid Power Fundamentals: Calculating Capacity and Net Revenue. *J. Power Sources* **2005**, *144*, 268–279. [CrossRef]
- Roccatelli, M.; Mangini, A.M. Advances on Smart Cities and Smart Buildings. *Appl. Sci.* **2022**, *12*, 631. [CrossRef]
- Huang, B.; Meijssen, A.; Annema, J.; Lukszo, Z. Are Electric Vehicle Drivers Willing to Participate in Vehicle-to-Grid Contracts? A Context-Dependent Stated Choice Experiment. *Energy Policy* **2021**, *156*, 112410. [CrossRef]
- Gong, S.; Cheng, V.H.S.; Ardeshiri, A.; Rashidi, T.H. Incentives and concerns on vehicle-to-grid technology expressed by Australian employees and employers. *Transp. Res. Part D Transp. Environ.* **2021**, *98*, 102986. [CrossRef]
- Guo, J.; Yang, J.; Lin, Z.; Serrano, C.; Cortes, A.M. Impact Analysis of V2G Services on EV Battery Degradation—A Review. In Proceedings of the 2019 IEEE Milan PowerTech, Milan, Italy, 23–27 June 2019.
- Steffen, T.; Fly, A.; Mitchell, W. Optimal electric vehicle charging considering the effects of a financial incentive on battery ageing. *Energies* **2020**, *13*, 4742. [CrossRef]
- Gao, Y.; Wang, C.; Wang, Z.; Liang, H. Research on Time-of-Use Price Applying to Electric Vehicles Charging. In Proceedings of the IEEE PES Innovative Smart Grid Technologies, Tianjin, China, 21–24 May 2012.
- Hutson, C.; Venayagamoorthy, G.K.; Corzine, K.A. Intelligent Scheduling of Hybrid and Electric Vehicle Storage Capacity in a Parking Lot for Profit Maximization in Grid Power Transactions. In Proceedings of the 2008 IEEE Energy 2030 Conference, Atlanta, GA, USA, 17–18 November 2008.
- Han, S.; Han, S.; Sezaki, K. Development of an Optimal Vehicle-to-Grid Aggregator for Frequency Regulation. *IEEE Trans. Smart Grid* **2010**, *1*, 65–72.
- Shi, W.; Wong, V.W.S. Real-Time Vehicle-to-Grid Control Algorithm under Price Uncertainty. In Proceedings of the 2011 IEEE International Conference on Smart Grid Communications (SmartGridComm), Brussels, Belgium, 17–20 October 2011.
- Yao, L.; Lim, W.H.; Tsai, T.S. A Real-Time Charging Scheme for Demand Response in Electric Vehicle Parking Station. *IEEE Trans. Smart Grid* **2017**, *8*, 52–62. [CrossRef]
- Meenakumar, P.; Aunedi, M.; Strbac, G. Optimal Business Case for Provision of Grid Services through EVs with V2G Capabilities. In Proceedings of the 2020 Fifteenth International Conference on Ecological Vehicles and Renewable Energies (EVER), Monte-Carlo, Monaco, 10–12 September 2020.
- Aldik, A.; Al-Awami, A.T.; Sortomme, E.; Muqbel, A.M.; Shahidepour, M. A Planning Model for Electric Vehicle Aggregators Providing Ancillary Services. *IEEE Access* **2018**, *6*, 70685–70697. [CrossRef]
- Pearre, N.S.; Ribberink, H. Review of Research on V2X Technologies, Strategies, and Operations. *Renew. Sustain. Energy Rev.* **2019**, *105*, 61–70. [CrossRef]
- Noel, L.; Zarazua de Rubens, G.; Kester, J.; Sovacool, B.K. Beyond Emissions and Economics: Rethinking the Co-Benefits of Electric Vehicles (EVs) and Vehicle-to-Grid (V2G). *Transp. Policy* **2018**, *71*, 130–137. [CrossRef]

25. Yang, Q.; Li, J.; Cao, W.; Li, S.; Lin, J.; Huo, D.; He, H. An Improved Vehicle to the Grid Method with Battery Longevity Management in a Microgrid Application. *Energy* **2020**, *198*, 117374. [CrossRef]
26. Zhang, K.; Xu, L.; Ouyang, M.; Wang, H.; Lu, L.; Li, J.; Li, Z. Optimal Decentralized Valley-Filling Charging Strategy for Electric Vehicles. *Energy Convers. Manag.* **2014**, *78*, 537–550. [CrossRef]
27. Mignoni, N.; Scarabaggio, P.; Carli, R.; Dotoli, M. Control frameworks for transactive energy storage services in energy communities. *Control. Eng. Pract.* **2023**, *130*, 105364. [CrossRef]
28. Venkatesan, K.; Govindarajan, U. Optimal power flow control of hybrid renewable energy system with energy storage: A WOANN strategy. *J. Renew. Sustain. Energy* **2019**, *11*, 015501. [CrossRef]
29. Lopes, J.A.P.; Soares, F.; Almeida, P.R. Integration of Electric Vehicles in the Electric Power System. *Proc. IEEE* **2011**, *99*, 168–183. [CrossRef]
30. Aghajani, S.; Kalantar, M. A Cooperative Game Theoretic Analysis of Electric Vehicles Parking Lot in Smart Grid. *Energy* **2017**, *137*, 129–139. [CrossRef]
31. Neyestani, N.; Damavandi, M.Y.; Godina, R.; Catalao, J.P. Integrating the Pevs' Traffic Pattern in Parking Lots and Charging Stations in Micro Multi-Energy Systems. In Proceedings of the 2016 51st International Universities Power Engineering Conference (UPEC), Coimbra, Portugal, 6–9 September 2016.
32. Kim, Y.-J.; Blum, D.H.; Xu, N.; Su, L.; Norford, L.K. Technologies and Magnitude of Ancillary Services Provided by Commercial Buildings. *Proc. IEEE* **2016**, *104*, 758–779. [CrossRef]
33. Rahman, M.S.; Hossain, M.J.; Lu, J.; Pota, H.R. A Need-Based Distributed Coordination Strategy for EV Storages in a Commercial Hybrid AC/DC Microgrid with an Improved Interlinking Converter Control Topology. *IEEE Trans. Energy Convers.* **2018**, *33*, 1372–1383. [CrossRef]
34. Yu, H.; Niu, S.; Shang, Y.; Shao, Z.; Jia, Y.; Jian, L. Electric Vehicles Integration and Vehicle-to-Grid Operation in Active Distribution Grids: A Comprehensive Review on Power Architectures, Grid Connection Standards and Typical Applications. *Renew. Sustain. Energy Rev.* **2022**, *168*, 112812. [CrossRef]
35. Yu, Y.; Nduka, O.S.; Pal, B.C. Smart Control of an Electric Vehicle for Ancillary Service in DC Microgrid. *IEEE Access* **2020**, *8*, 197222–197235. [CrossRef]
36. Zhou, T.; Sun, W. Research on Multi-objective Optimisation Coordination for Large-scale V2G. *IET Renew. Power Gener.* **2019**, *14*, 445–453. [CrossRef]
37. Rezaeimozafar, M.; Eskandari, M.; Savkin, A. A Self-Optimizing Scheduling Model for Large-Scale EV Fleets in Microgrids. *IEEE Trans. Ind. Inform.* **2021**, *17*, 8177–8188. [CrossRef]
38. Bui, V.-H.; Hussain, A.; Su, W. A Dynamic Internal Trading Price Strategy for Networked Microgrids: A Deep Reinforcement Learning-Based Game-Theoretic Approach. *IEEE Trans. Smart Grid* **2022**, *13*, 3408–3421. [CrossRef]
39. Bui, V.-H.; Hussain, A.; Kim, H.-M. A Multiagent-Based Hierarchical Energy Management Strategy for Multi-Microgrids Considering Adjustable Power and Demand Response. *IEEE Trans. Smart Grid* **2018**, *9*, 1323–1333. [CrossRef]
40. Umoren, I.A.; Jaffary, S.S.; Shakir, M.Z.; Katzis, K.; Ahmadi, H. Blockchain-Based Energy Trading in Electric-Vehicle-Enabled Microgrids. *IEEE Consum. Electron. Mag.* **2020**, *9*, 66–71. [CrossRef]
41. Lin, Y.; Wang, J. Realizing the Transactive Energy Future with Local Energy Market: An Overview. *Curr. Sustain. Energy Rep.* **2022**, *9*, 1–14. [CrossRef]
42. Su, J.; Zhang, Y.; Yang, C.; Xing, G.; Du, S. Price Demand Response Model Based on Consumer Psychology. In Proceedings of the 2020 IEEE 4th Conference on Energy Internet and Energy System Integration (EI2), Wuhan, China, 30 October–1 November 2020.
43. Xing, Y.; Li, F.; Sun, K.; Wang, D.; Chen, T.; Zhang, Z. Multi-Type Electric Vehicle Load Prediction Based on Monte Carlo Simulation. *Energy Rep.* **2022**, *8*, 966–972. [CrossRef]
44. Zhang, J.; Yan, J.; Liu, Y.; Zhang, H.; Lv, G. Daily Electric Vehicle Charging Load Profiles Considering Demographics of Vehicle Users. *Appl. Energy* **2020**, *274*, 115063. [CrossRef]
45. Zhou, K.; Cheng, L.; Wen, L.; Lu, X.; Ding, T. A Coordinated Charging Scheduling Method for Electric Vehicles Considering Different Charging Demands. *Energy* **2020**, *213*, 118882. [CrossRef]
46. Hussain, A.; Bui, V.-H.; Kim, H.-M. Optimal Sizing of Battery Energy Storage System in a Fast EV Charging Station Considering Power Outages. *IEEE Trans. Transp. Electrif.* **2020**, *6*, 453–463. [CrossRef]
47. Li, K.; Tseng, K.J. Energy Efficiency of Lithium-Ion Battery Used as Energy Storage Devices in Micro-Grid. In Proceedings of the IECON 2015—41st Annual Conference of the IEEE Industrial Electronics Society, Yokohama, Japan, 9–12 November 2015.
48. Hussain, A.; Kim, H.-M. Evaluation of Multi-Objective Optimization Techniques for Resilience Enhancement of Electric Vehicles. *Electronics* **2021**, *10*, 3030. [CrossRef]
49. Marler, R.T.; Arora, J.S. Survey of Multi-Objective Optimization Methods for Engineering. *Struct. Multidiscip. Optim.* **2004**, *26*, 369–395. [CrossRef]
50. IBM. IBM Documentation. 2023. Available online: <https://www.ibm.com/docs/en/icos/22.1.0?topic=optimizers-users-manual-cplex> (accessed on 2 May 2023).
51. Bashari, M.; Rahimi-Kian, A. Forecasting Electric Load by Aggregating Meteorological and History-Based Deep Learning Modules. In Proceedings of the 2020 IEEE Power Energy Society General Meeting (PESGM), Montreal, QC, Canada, 2–6 August 2020.
52. EV Database. “Range of Full Electric Vehicles”. Database, Electric Vehicle. 2022. Available online: <https://ev-database.org/> (accessed on 2 May 2023).

53. Ali, A.Y.; Hussain, A.; Baek, J.-W.; Kim, H.-M. Optimal Operation of Networked Microgrids for Enhancing Resilience Using Mobile Electric Vehicles. *Energies* **2020**, *14*, 142. [[CrossRef](#)]
54. Bui, Y.-H.; Hussain, A.; Kim, H.-M. Double Deep Q-Learning-Based Distributed Operation of Battery Energy Storage System Considering Uncertainties. *IEEE Trans. Smart Grid* **2020**, *11*, 457–469. [[CrossRef](#)]
55. Scarabaggio, P.; Carli, R.; Dotoli, M. Noncooperative equilibrium-seeking in distributed energy systems under AC power flow nonlinear constraints. *IEEE Trans. Control Netw. Syst.* **2022**, *9*, 1731–1742. [[CrossRef](#)]
56. Yao, M.; Molzahn, D.K.; Mathieu, J.L. An optimal power-flow approach to improve power system voltage stability using demand response. *IEEE Trans. Control Netw. Syst.* **2019**, *6*, 1015–1025. [[CrossRef](#)]

Disclaimer/Publisher’s Note: The statements, opinions and data contained in all publications are solely those of the individual author(s) and contributor(s) and not of MDPI and/or the editor(s). MDPI and/or the editor(s) disclaim responsibility for any injury to people or property resulting from any ideas, methods, instructions or products referred to in the content.